Balance perturbation and error processing elicit distinct brain dynamics

Journal of Neural Engineering

PAPER

Balance perturbation and error processing elicit distinct brain dynamics

Shayan Jalilpour[1] and Gernot Müller-Putz[1,2,*]

[1] Institute of Neural Engineering, Graz University of Technology, Graz, Austria
[2] BioTechMed, Graz, Austria
* Author to whom any correspondence should be addressed.

E-mail: gernot.mueller@tugraz.at

Keywords: electroencephalography, perturbation-evoked potential, error-related potential, source localization

Supplementary material for this article is available online

OPEN ACCESS

RECEIVED
8 November 2022

REVISED
2 March 2023

ACCEPTED FOR PUBLICATION
15 March 2023

PUBLISHED
31 March 2023

Abstract

Objective. The maintenance of balance is a complicated process in the human brain, which involves multisensory processing such as somatosensory and visual processing, motor planning and execution. It was shown that a specific cortical activity called perturbation-evoked potential (PEP) appears in the electroencephalogram (EEG) during balance perturbation. PEPs are primarily recognized by the N1 component with a negative peak localized in frontal and central regions. There has been a doubt in balance perturbation studies whether the N1 potential of perturbation is elicited due to error processing in the brain. The objective of this study is to test whether the brain perceives postural instability as a cognitive error by imposing two types of perturbations consisting of erroneous and correct perturbations. *Approach*. We conducted novel research to incorporate the experiment designs of both error and balance studies. To this end, participants encountered errors during balance perturbations at rare moments in the experiment. We induced errors by imposing perturbations to participants in the wrong directions and an erroneous perturbation was considered as a situation when the participant was exposed to an opposite direction of the expected/informed one. In correct perturbations, participants were tilted to the same direction, as they were informed. We analyzed the two conditions in time, time-frequency, and source domains. *Main results*. We showed that two error-related neural markers were derived from the EEG responses, including error positivity (Pe), and error-related alpha suppression (ERAS) during erroneous perturbations. Consequently, early neural correlates of perturbation cannot be interpreted as error-related responses. We discovered distinct patterns of conscious error processing; both Pe and ERAS are associated with conscious sensations of error. *Significance*. Our findings indicated that early cortical responses of balance perturbation are not associated with neural error processing of the brain, and errors induce distinct cortical responses that are distinguishable from brain dynamics of N1 potential.

1. Introduction

Understanding the complex process of balance control in the human brain is a pivotal step in learning the underlying brain mechanism of cognitive control and sensorimotor processing. With advancements in neuroimaging techniques, the studies of human neural activity during balance have received considerable attention, although our knowledge about real-life brain responses during postural perturbations is bounded. Electroencephalography (EEG) is the most used neuroimaging method to evaluate brain activity in response to balance perturbations because of its high temporal resolution and ease of recording. It has been shown that postural instabilities are preceded by a specific brain activity pattern called perturbation-evoked potential (PEP) dispersed over front-centro-parietal areas [1–6]. PEPs are composed of different EEG components, including a large negative peak (N1), followed by positive (P2)

and negative (N2) waves, respectively [7]. This EEG potential induced by whole-body perturbation has been studied under different paradigms, including surface perturbations [3, 8–10], platform translations [5, 8, 11–13], rotation [1, 4, 14], and weight-release [15–18]. PEPs are primarily recognized by N1 components with a negative peak between 85 and 163 ms, and localized in the frontal and central regions. The N1 component is an indicator of body postural perturbation irrespective of its cause, and it is observable in all types of balance destabilization. During postural instability, the cortex is involved in multisensory processing encompassed by visual, vestibular, and somatosensory systems that cause different parameters to regulate the perturbation-evoked responses. The evidence of multiple studies suggests that latency and amplitude of the N1 component are manipulated by physical characteristics of perturbation (i.e. intensity or velocity) [11, 19, 20], or by environmental and psychological characteristics of the experiment and participants [10, 21–23]. In the Dietz *et al* study [2], participants were subjected to random perturbations while they stood on a treadmill. Postural displacement was produced in two conditions consisting of self-induced and experimenter-induced perturbations. They found out that the magnitude of N1 decreased significantly when the participants induced the perturbations by themselves. They concluded that the changes in neural responses between predictable and unpredictable perturbations reflect a link between the N1 potential and the error detection process. Adkin *et al* [21] explored the aspect of the postural threat of N1 components for predictable and unpredictable trunk perturbations. They operated postural threat by conducting the experiment on an elevated surface located 3.2 m above the ground level. The cortical responses were evaluated at the low and high surface height conditions with the same force perturbation. They showed that the amplitude of the N1 component in high conditions was increased significantly compared with low height conditions for unpredictable perturbations. Also, no perturbation evoked activity appeared in the predictable perturbation. Goel and colleagues [11] examined the effect of support surface translations in two different directions (backward and forward) and speeds (high and low). They reported that the amplitude of N1 was significantly larger for high-speed perturbation compared with low-speed ones. Additionally, no differences were found in the N1 peak amplitude and latency as a function of the perturbation direction. In our previous study [24], it was shown that the modulation of cortical responses elicited by balance perturbation carries direction- and angle-specific information which can be classified with reliable accuracy. In another study by Adkin and colleagues [22], they applied displacement in predictable and unpredictable manners. In their experiment, participants experienced transient horizontal perturbations to the trunk while they maintained an upright stance with closed eyes. A large negative potential emerged for unpredictable perturbations, whereas no discernible N1 component was diagnosed during the predictable perturbations. They argued that N1 potentials represent a function of error processing in unexpected stimulation.

Payne and colleagues [25] compared the relevant studies to balance control and cognitive error detection studies, and they suggested that the N1 component elicited in response to balance perturbation shows analogous neural activity to the classical error-related negativity (ERN). The ERN or error negativity (Ne) is a cortical response to erroneous action [26–28], which appears around 50 ms after an error commission over frontocentral electrodes [29]. This negativity arises from the medial-frontal cortex (MFC) especially in the anterior cingulate cortex (ACC) [30–32], and it is evoked when participants commit a mistake in forced-choice speeded response paradigms. Commonly used tasks to elicit error brain responses include the flanker task [29, 33, 34], go/no-go task [35–38], and stroop task [39–41].

The other EEG component that occurs during error processing is a positive potential called Pe. It is a parietal positive deflection that is maximized around 200–500 ms after the error onset [26, 31]. Moreover, Pe is hypothesized to catch the higher level characteristic of error processing, and it is linked to error awareness [42–44]. Pe and P300 originate from the same source with respect to the time course and scalp topographies [45, 46].

Albeit, it is assumed that the ERN and balance N1 show similar neural patterns, and they scale with similar factors of stimulation (e.g. predictability of perturbation or error [29, 47], and perceived consequence of perturbation or error [19, 48]), there is still ambiguity that how these two EEG potentials are related. ERN and PEP come from different sources; the N1 potential of PEP is localized in the supplementary motor area (SMA) [11, 49–51], while the ERN appears in the cingulate cortex (especially ACC) [29, 52–56]. Although both areas are localized in the pMFC, the research indicated that pMF acts as a 'neural alarm' and is responsive to a broad range of elicitors such as performance monitoring and adjustments, the detection of an error, anomalies, discrepancies, adverse outcomes, and decision uncertainty [30, 57–59].

Moreover, in the error-relevant studies, an ErrP was generated in an experimental task where participants perceived the wrong action at some rare moments during the experiment- in this situation either participants make an error or observe an error. Therefore, false information is conveyed to the participants, which is in contradiction to the expected outcome. In balance studies, participants expect

the destabilizing event in the experiment even in scenarios with unpredictable perturbations, and consequently, no wrong information leads to a misinterpretation during perturbation.

In this work, we tested whether the brain perceives postural instability as a cognitive error by imposing two types of perturbations consisting of error and correct perturbations. We hypothesize that the N1 component or the general loss of balance is not attributed to error detection. Two types of perturbations were generated by incorporating the experiment designs of both error and balance studies. To this end, participants were tilted to the wrong or correct direction in the experiment. Wrong perturbation is considered as a situation when the participant was exposed to an opposite direction of the expected/informed one, which led to encountering errors. This experimental paradigm permits us to directly study whether the N1 is representative of error processing.

2. Methods

2.1. Participants

Sixteen healthy individuals (age: 21–28 years; 7 females) participated in the study with monetary compensation for their participation. Data of one participant was excluded from analysis due to the data corruption. All participants had normal vision without a history of neurological disorders. One participant was excluded because of missing data. The study was approved by the Medical University of Graz, and all the participants signed written informed consent before the experiment.

2.2. Task paradigm and experimental procedure

Participants sat in a glider (Ka 8b, Alexander Schleicher GmbH & Co. Segelflugzeugbau) facing a computer screen at a distance of 1 m. We used a KUKA KRC1 robot (Kuka AG, Augsburg, Germany) to impose unpredictable balance perturbations by off-vertical axis rotation (OVAR) at tilting angles of 5°. The perturbations were presented in the form of sudden movement and tilted the glider in the left and right directions. The direction of perturbations was shown on the screen between 2 and 4 s before the perturbation onset, unequal intervals were selected to decrease the predictability of perturbations. Subjects were instructed to place their hand on the immovable control stick, and focus on the screen. Each trial consisted of one time tilting the glider to the left or right direction at high speed, and an interstimulus interval of 4–7 s was used to separate the consecutive perturbations. At the start of the experiment, directional cues were presented in gray arrows on the screen, and the glider was in a stable position. One directional cue (arrow) turned to green between 2 and 4 s before the perturbation onset to notify the subjects about the upcoming direction of the movement. Then, the sign's color changed to gray after the perturbation and stayed the same until the next trial. We name a trial as an error when the perturbation's direction did not coincide with the directional arrow. After the perturbation, the glider remained stationary for 2 s at the tilted position, and after that, it returned to the initial position slowly. Participants performed six blocks of 50 trials; 20% trials were error trials (60 trials) and the remaining 80% were correct trials (240 trials). Participants experienced ten error trials in each block; both the order and direction of errors were randomized throughout the experiment. A schematic of the experiment is depicted in figure 1.

2.3. EEG acquisition

We measured EEG signals using 63 active shielded Ag/AgCl electrodes located according to the international 10–5 electrode system (eego sports, ANT-neuro, Enschede, Netherlands). The data were sampled at 512 Hz with reference and ground placed at CPz and AFz, respectively. We recorded the exact positions of the EEG electrodes for each individual using an ELPOS Digitizer (Zebris Medical). To detect the perturbation onset, we measured the acceleration of the movements sampled at 500 Hz. The acceleration data were synchronized with the EEG data using the Lab Streaming Layer [60]. The accelerometer was mounted on the top part of the glider.

2.4. EEG preprocessing

Preprocessing was done using EEGLAB [61], BrainStorm [62], and fieldtrip software [63]. EEG data were bandpass filtered between 0.5 and 40 Hz, and downsampled to 256 Hz. We rejected the noisy channels which had a kurtosis higher than 5 or were correlated less than 75% with neighborhood channels. To eliminate noisy parts of the data, we applied artifact subspace reconstruction [64] and reconstructed the artificial parts by using clean EEG data. A threshold of 20 SDs was selected, which is consistent with previous balance studies [17, 65, 66]. Next, we performed independent component analysis (ICA) on each block of the experiment. Additionally, individualized channel locations obtained from the Zebris device were used for running ICA. ICLabel was exploited to determine the origin of components in the brain, heart, muscles, eyes, or other sources [67]. Subsequently, the artifact-related independent components were removed if they had a probability higher than 80%, and then the data were reconstructed with the remaining components. Finally, the cleaned data were referenced to the common average reference (CAR), and the removed channels were interpolated from neighboring electrodes using spherical spline interpolation. After implementing the preprocessing pipeline on each block, we extracted 1.5 s epochs with respect to perturbation onset obtained from accelerometer data. We excluded the noisy epochs by using

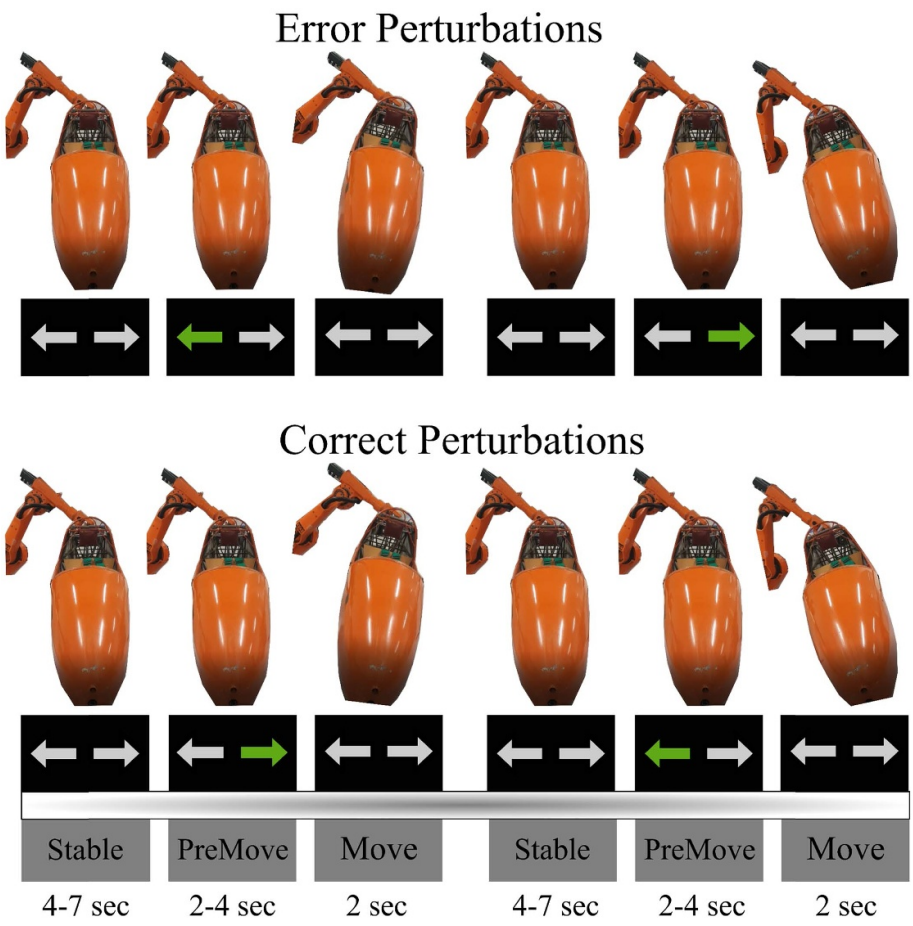

Figure 1. Schematic of the paradigm (four trials). One trial started with a stable position, after 5–8 s participants were informed about the direction of movement, then they were tilted to the opposite (error trial) or same (correct) direction. The glider stayed in the tilted position for 2 s, and then it returned to its stable position with a low speed.

the three different statistical parameters (abnormal amplitude, kurtosis, and joint probability).

2.5. Time-domain analysis

For electrophysiological analysis, we firstly investigated the amplitude changes of stimulus-evoked activity in the time domain. Each trial was baseline-corrected by subtracting the mean of the interval of 500–100 ms before the perturbation onset. For each condition, trials were averaged separately among the participants. Then, a two-sided cluster-based permutation [68] test (2000 times) with an alpha level of 0.025 was implemented on averaged signals with a final sample size of 15 participants. A *p*-value of 0.025 was considered to determine the significance of the ERP difference between the two conditions. Additionally, t-statistics were computed to indicate the ratio of the difference between the two classes.

2.6. Time-frequency analysis

To assess the neural correlates of non-phase-locked activities independent of phase-locked evoked potentials in the time-frequency domain, we calculated event-related spectral perturbation (ERSP) by using the intertrial variance [69]. In this way, we unmasked the effect of ERP from EEG desynchronization or synchronization. A Morlet Wavelet transformation was applied on each single trial EEG with a length of 2 s (0.5 s before to 1.5 s after perturbation onset). The wavelet cycles begin with one cycle at the lowest frequency, and it increases linearly until the highest frequency. The frequency range was chosen between 2 and 40 Hz, and the baseline activity was subtracted in the interval of 500–100 ms preceding perturbation onset. This leads to 50 logarithmic frequency bins and 200 linear time bins. Next, we performed the cluster-based permutation test, corrected by a 2000 random permutation test with a p level of 0.025.

2.7. Source-space analysis

EEG source imaging was performed for each participant and condition using the Brainstorm toolbox [62]. The ICBM152 boundary element model (BEM) was utilized to register the template head model to the individual EEG electrode positions recorded by the Zebris device. A three-shell BEM (cortex, skull, scalp) with conductivities of 0.41, 0.02, and 0.47 was exploited to estimate the lead field matrix with OpenMEEG [70]. The noise covariance matrix was computed by considering the time window

of 500–100 ms before the perturbation onset. The cortical sources were estimated via Minimum Norm Estimation, using sLORETA [71] with unconstrained dipole orientation. We have a current density distribution consisting of 15 002 dipole locations. Additionally, the obtained dipoles were segmented into 68 parcels based on the Desikan-Kiliani atlas. For each parcel, the activity of all voxels within that specified region was averaged to indicate the parcel's time course of activity. For the statistical test, we found significant neural sources among error and correct perturbations using a cluster-based permutation test (paired-sample, $\alpha = 0.025$, 2000 permutations).

3. Results

In the following, we first provide the analysis results in the time domain by the comparison of phase-locked EEG components. Then, we explore non-phase-locked responses in the time-frequency domain by computing the ERSP of error and correct trials. Ultimately, to explore the relationships between neural sources, we present the results of the source domain.

3.1. Time-domain results: event-related potentials

To attain insight into event-related potentials, the statistical test was performed on time domain signals; we represented the *t*-values in figure 2. We created eight clusters to show the different regions of the brain. These regions comprised of pre-frontal, frontal, fronto-central, central, centro-parietal, parietal, occipital, and temporal areas. As can be seen, frontal, central, and parietal areas disclosed significant differences between the conditions. In figure 2, positive values of the *t*-value indicate that the amplitude of the error condition was significantly greater than the correct condition, and negative values denote that the significant samples in the error condition were smaller than the other condition. The obtained results show that prominent differences occurred in the 200–500 ms interval. Moreover, the grand averaged signal of Pz electrode was plotted in the upper panel of figure 2 to display perturbation-evoked responses of error and correct conditions.

Then, we took the average of the *p*-values for each channel and gained the most discriminable electrodes. Figure 3 shows the grand average stimulus-evoked activity for electrodes CCP1h, POz, Pz, and CP1, which are the most important EEG channels. We also plotted the average error-minus-correct difference waveform (difference between averaged responses of erroneous and correct perturbations).

The EEG potentials in both conditions exhibited negative and following positive peaks around 50–110 and 150–300 ms. These two peaks are characterized by N1 and P2 components common in balance perturbation studies. The reverse polarity in POz and Pz electrodes appeared because of the referencing, as we used CAR instead of CPz channel. We see similar activities of the N1 potential for both correct and error trials, while the overall waveform shape of P2 is more pronounced in error perturbations. The difference waveform resulted in a notable positivity around 200–500 ms.

Topographical maps of averaged erroneous, correct, and different signals with the accompaniment of *p*-value scalp topographies are shown in figure 4. The spatial distribution of electrophysiological activity at different time points, including the onset of the perturbation and the N1 peak is illustrated there. It is visible that no significant differences were found in N1 potentials between correct and error trials, suggesting that this component is attributed to the loss of balance, not error-related processing. Frontal areas show larger negative modulation in the correct condition at 250 ms, while the parietal positive activity seems identical in both classes. Between 300 and 500 ms, the error class manifests higher positivity in parietal channels, and they are significantly different over parietal and occipital regions. Additionally, error and correct classes have significant differences over frontal channels at 430 ms, and error condition shows greater negativity in this area. The brain responses did not reveal any statistical difference between the two classes between 700 and 1300 ms.

3.2. Time-frequency results

We statistically investigated the time-frequency activity of erroneous and correct classes using the cluster permutation test. Figure 5 depicts the difference plot between the averaged ERSP of error and correct trials (error-minus-correct) of important channels, the black frame inside the plots specifies significant differences. The ERSP of all channels were plotted in figure 1 of supplementary material.

It can be seen that the alpha (7.5–13 Hz) frequency band de-synchronized after the perturbation onset in the time range of 500–830 ms over the central parts of the left hemisphere. As shown in figure 5, large desynchronization of ERSPs is prevalent in the C3, CCP3h, CP3, C1, FCC3h, FC3, CP1, FCC1h, FC1, CCP1h, FCz, FC5, C5, FCC2h, and Cz electrodes. To have a better intuition about the time-frequency characteristics of EEG signals, we plotted the ERSP of each condition separately for the aforementioned electrodes in figure 6.

3.3. Source space results

In order to represent the sources of perturbations and error processing, we visualized the entire 68 regions of the Desikan-Kiliani atlas for both conditions in figure 7. EEG activity increased under both conditions between 100 and 150 ms in the SMA, especially in the paracentral and posterior cingulate which is the cortical source of physical perturbations. No significant results were found in early neural responses of perturbation between the two conditions, which

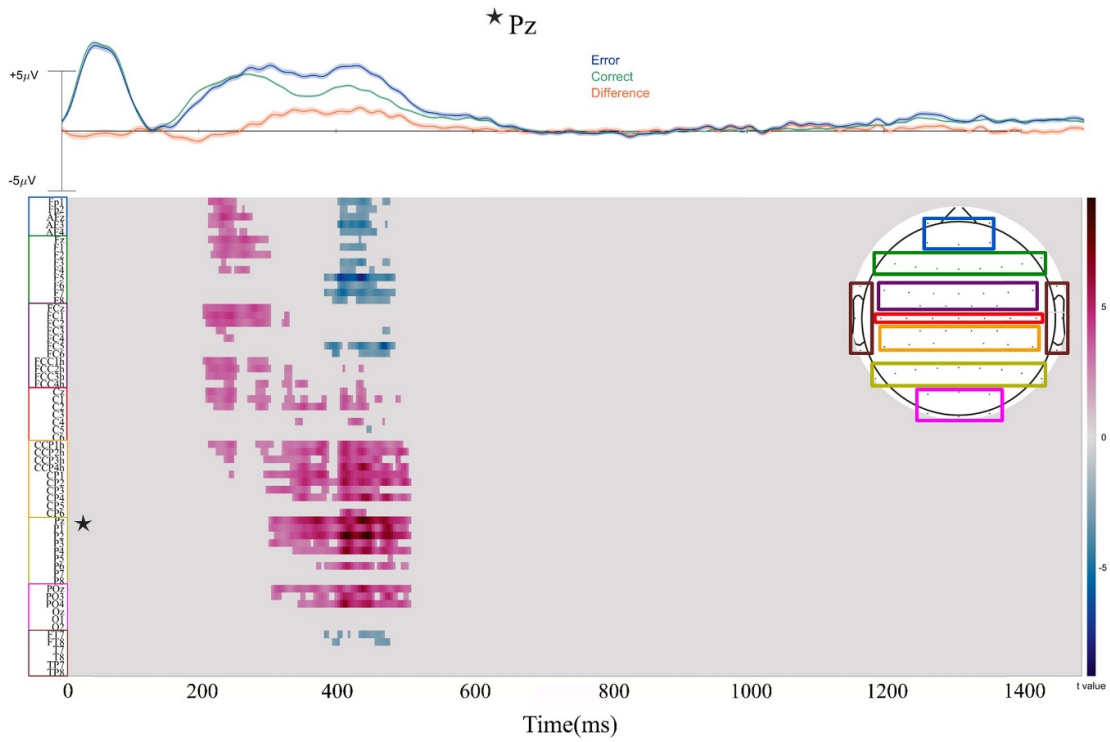

Figure 2. Time domain t-value plot. Positive and negative values indicate a forward and reversal relation between two classes. Each line represents one channel. We assigned eight clusters to different parts of the brain so that blue, green, purple, red, orange, pink and brown colors represent pre-frontal, frontal, fronto- central, central, centro-parietal, parietal, occipital and temporal areas. The EEG potential at Pz was plotted in the upper part of the figure, and its t- value row was marked by a black star in the t-value plot.

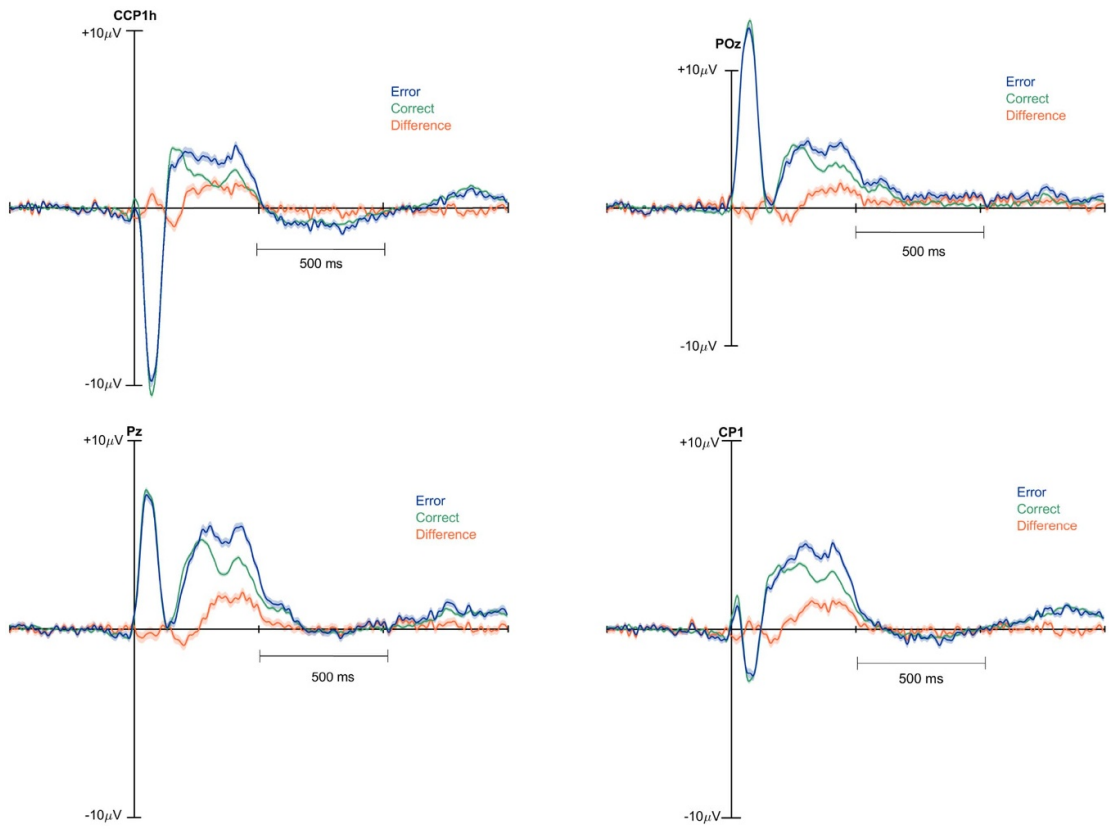

Figure 3. Average EEG responses of error trials, correct trials and error-minus-correct signals across 15 participants over CCP1h, POz, Pz and CP1 channels. The blue and green lines characterize the error and correct conditions, in addition to the orange plot as the indicator of difference signal.

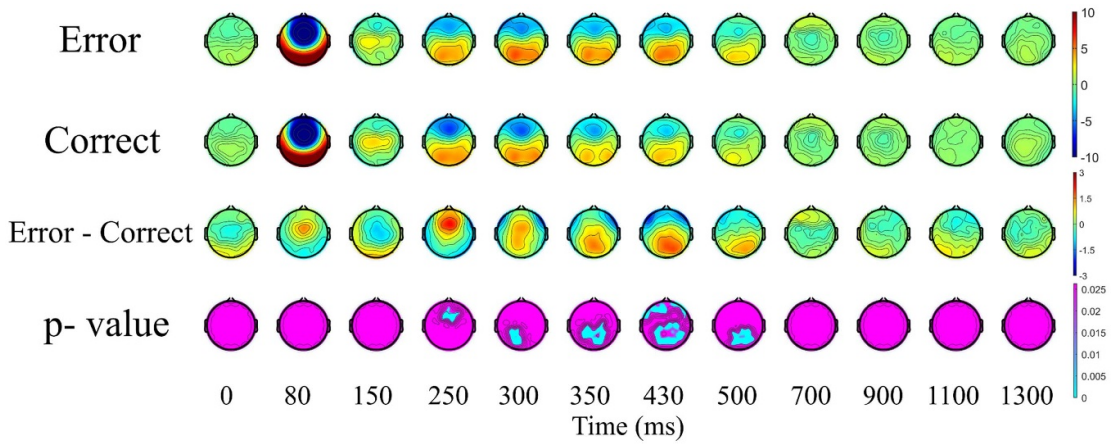

Figure 4. Grand averaged scalp topography. EEG distribution of error, correct and error-correct is plotted in the first, second and third rows, respectively. The last row depicts *p*-values results of the statistical analysis.

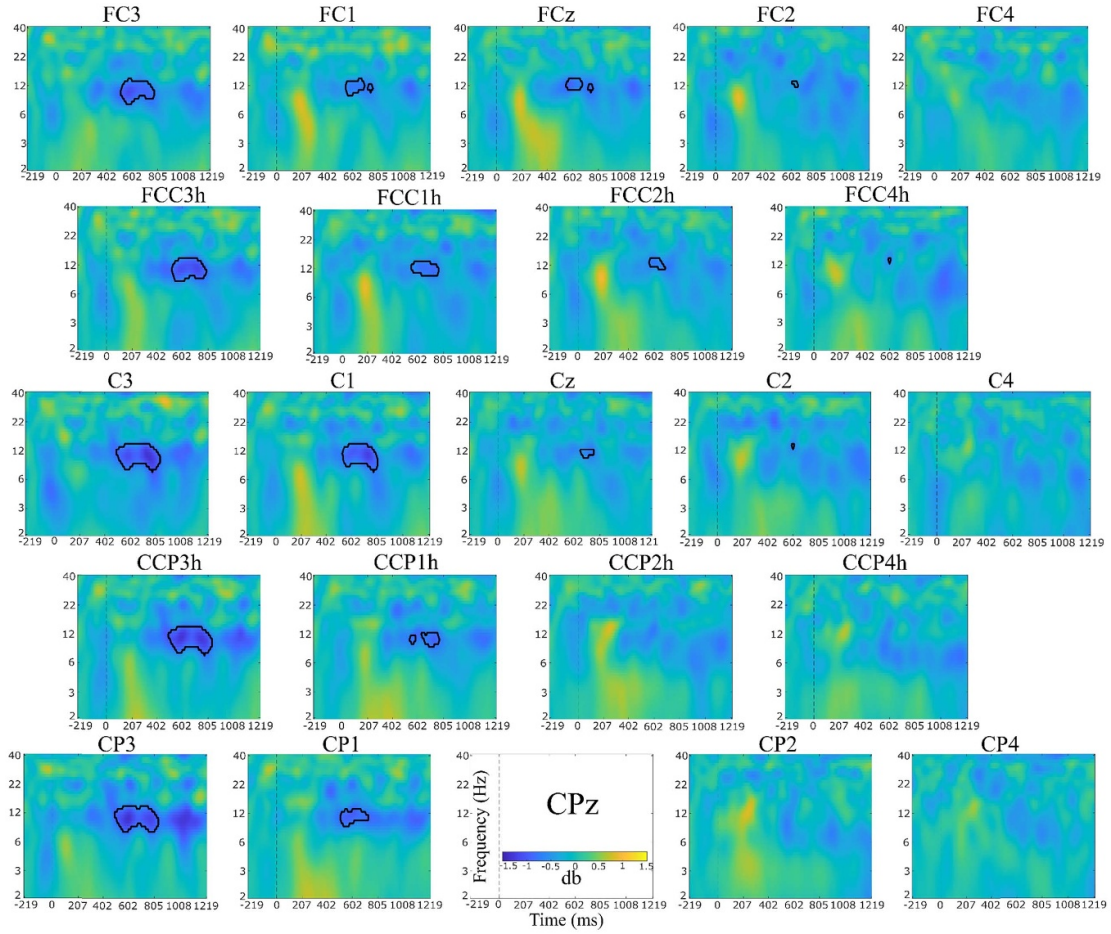

Figure 5. ERSP differences are shown for important channels. Significant reduction in alpha power frequency is observable over central channels.

reveals that N1 potential comes from the same source in both error and correct perturbations.

In the time interval of 250–500 ms, it can be seen that the grand average activity is predominant in the parietal and occipital regions, for both classes. We found significant activations in the inferior parietal L, isthmus cingulate L, and superior parietal L areas in the time range of 280–470 ms, and the activity became stronger in error trials. We did not discover a significant activity between 430 and 900 ms, and both conditions displayed analogous behavior in this period. At 1100 ms, the fusiform parcel represents greater activation for error trials, which is visible in the difference source plot.

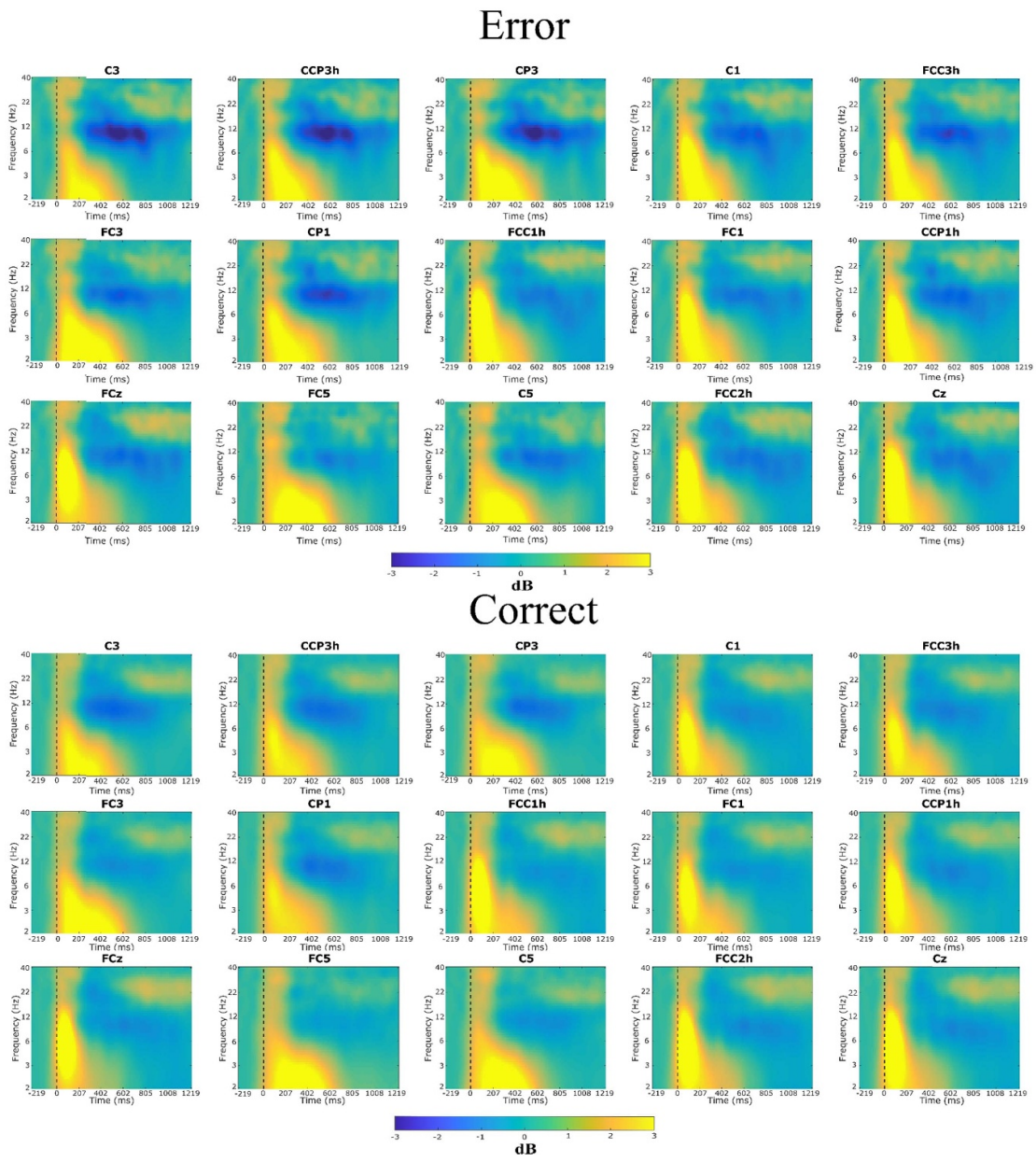

Figure 6. Averaged ERSP plot of 15 participants scaled power in dB. Plots of error and correct trials were displayed separately for channels C3, CCP3h, CP3, C1, FCC3h, FC3, CP1, FCC1h, FC1, CCP1h, FCz, FC5, C5, FCC2h and Cz.

4. Discussion

This study aimed to explore the dynamics of the brain during the occurrence of an error in balance perturbation. In previous studies, it was revealed that the early cortical negativity is elicited by postural changes in brain responses to the realization of perceived instability. Several studies have suggested that this negativity shares similar traits with ErrP in terms of the spatial and temporal characteristics of N1 potentials [22, 25, 72]. It has been shown that different cortical sources will be activated in the elicited negative potential of ErrP and PEP. The N1 potential of PEP is localized in the SMA [11, 49–51], while the ERN of ErrP appears in the ACC [29, 52–56]. As these areas are localized in the pMFC, it has been proposed that the negative component of the PEP and the ErrP represent different aspects of error monitoring. Studies on error processing have demonstrated that ErrP signals occur under different task situations, and they are generated in various contexts of the perception of wrong action. Feedback ErrP happens when the participant realizes the wrong feedback on the task [73]. The term interaction ErrP is used when the participant interacts with a brain–computer interface (BCI), and the system delivers the false command [54, 74]. Observation ErrP is considered when the participant recognizes the machine's erroneous action [75]. Response ErrP is defined as a situation in which a participant commits an error by him/herself in a choice reaction time task [76]. The reported results manifest distinct shapes and latencies

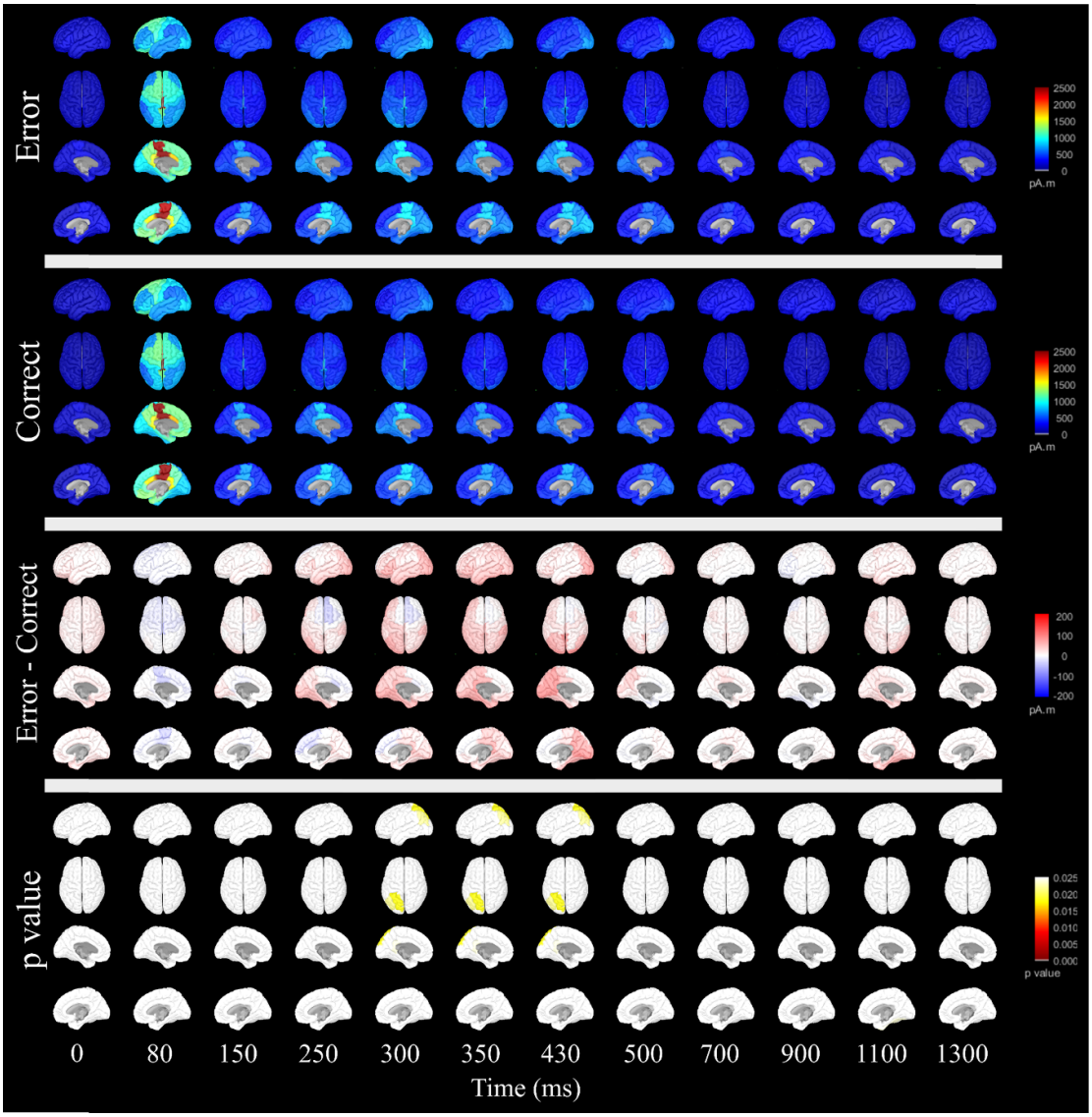

Figure 7. Grand-averaged EEG potentials of the source activations. The first and second panels show the grand-average source space activity for the error and correct conditions, respectively. Error-minus-correct activity of the source space is plotted on the third panel. The corresponding *p*-values obtained by a two- sided cluster permutation statistical test are displayed in the last panel.

of ErrP for different paradigms, while there is not any unique and clear explanation for those differences. However, some studies deduced that this disparity is probably attributed to the various experimental paradigms and required cognitive efforts to evaluate the task.

Numerous study designs were accomplished to yield perturbation such as platform translations [5, 8, 11–13], surface perturbation [3, 8–10], and weight release [15–18]. In all scenarios of balance studies, participants were instructed about the occurrence of the perturbation, and they were aware of balance destabilization in the experiment. Therefore, no wrong information was delivered to the subjects during the perturbation. While in error research, neural error responses were elicited by wrong recognition of action due to the paradox between intended and actual response (feedback). In this work, we designed a novel experimental paradigm inspired by error and balance studies so that participants confront unexpected movement errors during balance perturbation. In one experimental condition, participants experienced perturbations in a direction incongruent with the presented direction. In the other condition, they were tilted in the same direction as the informed direction. We delved into the brain mechanisms of error commission during the erroneous movement. We provided evidence that erroneous movements can be differentiated from correct movements with significant cortical changes.

4.1. Physiology

In this study, two types of cortical responses were evoked with respect to two stimuli (physical perturbation and error commission). To assess the differences between the two conditions, we mainly interpret the results by using the EEG difference waveform. Therefore, we can eliminate the common activities within

conditions, which are probably the brain dynamics of perturbations.

The difference plot did not yield a significant divergence between the N1 potentials of the two conditions. As figure 2 shows, error and correct trials are not different from each other in the time period of 0–200 ms. The distinct activities appeared over the frontal and central channels between 200 and 300 ms. When looking at the EEG potentials of the error and correct trials separately, we notice that both correct and error trials represent positive activities at this interval. Nevertheless, the error condition prolonged more than the correct condition, and the fluctuations arise due to the strong response of error perturbations.

The positive activity shifted from frontal areas to parietal regions between 250 and 500 ms, as is noticeable in figures 2 and 3. At 430 ms, the differences were maximized with negativity and positivity over the frontal and parietal regions, respectively. The temporal and topographical features of the EEG potential at this time point can be interpreted as an electrophysiological marker of conscious perception of errors called error positivity (Pe) [26]. Both error and correct classes demonstrate analogous neural correlates between 500 and 1300 ms, and the activity of both classes is close to zero in the time range.

4.2. Time-frequency

Moreover, we examine the spectral properties of error and correct trials by calculating the ERSP of signals. To this end, we exploited the intertrial variance method to eliminate the phase-locked activities of EEG. Figure 5 represents the difference ERSP plot (error minus correct), and error-related frequency modulation is remarkable in the alpha band within 500–830 ms (maximized between 575 and 595 ms). Also, figure 1-supplementary demonstrates that sub components of delta (2–3.5 Hz) and theta (3.5–6 Hz) frequency bands in the frontal channels synchronized after the perturbation onset in the time range of 400 and 600 ms. This effect was observed during error processing in numerous studies [77–80], but no significant differences were found in the statistical test of this study. In addition, spectral suppression was significantly evident in the central regions, especially in the left side of the hemisphere. This phenomenon is named error-related alpha suppression (ERAS) [81, 82], which refers to the reduction of alpha power in an error condition with respect to the correct condition. Since the decrease of alpha band is an indicator of attentional demands such as alertness [83], ERAS reflects higher attention needs of the participant in the errors than correct trials [84] Moreover, this post-error compensation only appears in aware error responses when the participants are conscious and alert of error commission [85]. Our obtained results are in agreement with previous studies that showed a power decrease in the alpha band [81, 82, 86, 87]. To further investigate the frequency modulations, we plotted the time frequency decomposition of the error and correct classes separately. The analysis of both conditions revealed that the first spectral peak happened during the PEP N1 in the delta, theta, alpha, and beta frequency bands. This response is followed by a power decrease in the alpha band for error trials over left central regions. The frequency modulation of the left hemisphere is probably attributed to the handedness of the participants. Fourteen of 15 participants were right-handed, and we speculate that errors were more unpleasant for right-handed participants during the left balance perturbation.

4.3. Source analysis

Through source analysis, we showed that there is no significant difference between the activated sources of N1 between error and correct conditions. Although we expected to see greater amplitude (activation) on N1 for error perturbations, the results confirm that the N1 potential is independent of error processing and it primarily contributes to the physical characteristics of perturbation. The significant activation originates from the superior parietal, inferior parietal, and isthmus cingulate, with the maximum differences at 430 ms. By looking at error and correct sources, we find higher source activity for error perturbation in the time interval of 250–500 ms. These areas play an important role in error processing, and they are probably attributed to error positivity. Neuroimaging studies investigating errors reported that the sustained activity of the posterior cingulate relates to the emergence of a Pe. By inspection of the source and time domain results at 430 ms, we can imply that the EEG potential reflects the same traits of error-related positivity or Pe. It is known that Pe is attributed to error awareness and post error processing [88–90].

Moreover, the fusiform gyrus had stronger activation during errors than the correct class around 1100 ms. The existence of fusiform gyrus activation in error processing was reported in a stop task during functional magnetic resonance imaging [91]. Albeit we did not find any significant activity modulation in the time and time-frequency domains at this time point.

5. Conclusion

To sum up, we demonstrate a novel study to expand the knowledge of cortical responses during balance by investigating the influence of error perturbation on the N1 potential and other EEG responses. In our approach, we induced errors by exposing perturbations to participants in the wrong directions, and participants perceived these perturbations as wrong actions or movements. Our results showed that two error-related neural markers were derived from the EEG responses, including error positivity (Pe), and

ERAS. Although balance perturbation causes a large negative amplitude of N1, there were no discernible distinctions between the correct and erroneous perturbations, as indicated by these findings. Consequently, early neural correlates of perturbation cannot be interpreted as error-related responses. We discovered distinct patterns of conscious error processing; both Pe and ERAS are associated with conscious sensations of error. As it was seen, the absence of the third error-related indices was noticed in the analysis. A possible reason for this phenomenon is that the ERN mainly contributed to the motor response execution, while in this work, participants did not commit an error.

Data availability statement

The data cannot be made publicly available upon publication because they are not available in a format that is sufficiently accessible or reusable by other researchers. The data that support the findings of this study are available upon reasonable request from the authors.

CRediT authorship contribution statement

Shayan Jalilpour: Idea, Design of the experimental study, Data acquisition, Formal analysis, Writing—original draft, Writing—review & editing. Gernot R. Müller-Putz: Design of the experimental study, Writing—review & editing.

Conflict of interest

The authors declare that they have no known competing financial interests or personal relationships that could have appeared to influence the work reported in this paper. This work was supported by TU Graz Open Access Publishing Fund. We would also like to appreciate members of the Institute of Neural Engineering for their fruitful comments regarding data processing and analysis.

ORCID iD

Gernot Müller-Putz https://orcid.org/0000-0002-0087-3720

References

[1] Ackermann H, Diener H C and Dichgans J 1986 Mechanically evoked cerebral potentials and long-latency muscle responses in the evaluation of afferent and efferent long-loop pathways in humans *Neurosci. Lett.* **66** 233–8
[2] Dietz V, Quintern J, Berger W and Schenck E 1985 Cerebral potentials and leg muscle e.m.g. responses associated with stance perturbation *Exp. Brain Res.* **57** 348–54
[3] Dietz V, Quintern J and Berger W 1984 Cerebral evoked potentials associated with the compensatory reactions following stance and gait perturbation *Neurosci. Lett.* **50** 181–6
[4] Dimitrov B, Gavrilenko T and Gatev P 1996 Mechanically evoked cerebral potentials to sudden ankle dorsiflexion in human subjects during standing *Neurosci. Lett.* **208** 199–202
[5] Duckrow R B, Abu-Hasaballah K, Whipple R and Wolfson L 1999 Stance perturbation-evoked potentials in old people with poor gait and balance *Clin. Neurophysiol.* **110** 2026–32
[6] Staines R W, McIlroy W E and Brooke J D 2001 Cortical representation of whole-body movement is modulated by proprioceptive discharge in humans *Exp. Brain Res.* **138** 235–42
[7] Varghese J P, McIlroy R E and Barnett-Cowan M 2017 Perturbation-evoked potentials: significance and application in balance control research *Neurosci. Biobehav. Rev.* **83** 267–80
[8] Bogost M D, Burgos P I, Little C E, Woollacott M H and Dalton B H 2016 Electrocortical sources related to whole-body surface translations during a single- and dual-task paradigm *Front. Hum. Neurosci.* **10** 524
[9] Nørgaard J E, Andersen S, Ryg J, Stevenson A J T, Andreasen J, Danielsen M B, Oliveira A, de S C and Jørgensen M G 2022 Effects of treadmill slip and trip perturbation-based balance training on falls in community-dwelling older adults (STABILITY): study protocol for a randomised controlled trial *BMJ Open* **12** e052492
[10] Palmer J A, Payne A M, Ting L H and Borich M R 2021 Cortical engagement metrics during reactive balance are associated with distinct aspects of balance behavior in older adults *Front. Aging Neurosci.* **13** 684743
[11] Goel R, Ozdemir R A, Nakagome S, Contreras-Vidal J L, Paloski W H and Parikh P J 2018 Effects of speed and direction of perturbation on electroencephalographic and balance responses *Exp. Brain Res.* **236** 2073–83
[12] Mihara M, Miyai I, Hatakenaka M, Kubota K and Sakoda S 2008 Role of the prefrontal cortex in human balance control *NeuroImage* **43** 329–36
[13] Solis-Escalante T, De Kam D and Weerdesteyn V 2020 Classification of rhythmic cortical activity elicited by whole-body balance perturbations suggests the cortical representation of direction-specific changes in postural stability *IEEE Trans. Neural Syst. Rehabil. Eng.* **28** 2566–74
[14] Ditz J C, Schwarz A and Müller-Putz G R 2020 Perturbation-evoked potentials can be classified from single-trial EEG *J. Neural Eng.* **17** 036008
[15] Mochizuki G, Sibley K M, Cheung H J, Camilleri J M and McIlroy W E 2009 Generalizability of perturbation-evoked cortical potentials: independence from sensory, motor and overall postural state *Neurosci. Lett.* **451** 40–44
[16] Mochizuki G, Sibley K M, Esposito J G, Camilleri J M and McIlroy W E 2008 Cortical responses associated with the preparation and reaction to full-body perturbations to upright stability *Clin. Neurophysiol.* **119** 1626–37
[17] Peterson S M and Ferris D P 2018 Differentiation in theta and beta electrocortical activity between visual and physical perturbations to walking and standing balance *Eneuro* **5** ENEURO.0207–18.2018
[18] Sibley K M, Mochizuki G, Frank J S and McIlroy W E 2010 The relationship between physiological arousal and cortical and autonomic responses to postural instability *Exp. Brain Res.* **203** 533–40
[19] Payne A M and Ting L H 2020 Worse balance is associated with larger perturbation-evoked cortical responses in healthy young adults *Gait Posture* **80** 324–30
[20] Solis-Escalante T, Stokkermans M, Cohen M X and Weerdesteyn V 2021 Cortical responses to whole-body balance perturbations index perturbation magnitude and predict reactive stepping behavior *Eur. J. Neurosci.* **54** 8120–38
[21] Adkin A L, Campbell A D, Chua R and Carpenter M G 2008 The influence of postural threat on the cortical response to

unpredictable and predictable postural perturbations *Neurosci. Lett.* **435** 120–5
[22] Adkin A L, Quant S, Maki B E and McIlroy W E 2006 Cortical responses associated with predictable and unpredictable compensatory balance reactions *Exp. Brain Res.* **172** 85–93
[23] Payne A M, McKay J L and Ting L H 2022 The cortical N1 response to balance perturbation is associated with balance and cognitive function in different ways between older adults with and without Parkinson's disease *Cereb. Cortex Commun.* **3** tgac030
[24] Jalilpour S and Müller-Putz G 2022 Toward passive BCI: asynchronous decoding of neural responses to direction- and angle-specific perturbations during a simulated cockpit scenario *Sci. Rep.* **12** 6802
[25] Payne A M, Ting L H and Hajcak G 2019 Do sensorimotor perturbations to standing balance elicit an error-related negativity? *Psychophysiology* **56** e13359
[26] Falkenstein M, Hohnsbein J, Hoormann J and Blanke L 1991 Effects of crossmodal divided attention on late ERP components. II. Error processing in choice reaction tasks *Electroencephalogr. Clin. Neurophysiol.* **78** 447–55
[27] Gehring W J, Liu Y, Orr J M and Carp J 2012 The error-related negativity (ERN/Ne) *The Oxford Handbook of Event-Related Potential Components* (Oxford: Oxford University Press) pp 231–91
[28] Gehring W J, Goss B, Coles M G H, Meyer D E and Donchin E 1993 A neural system for error detection and compensation *Psychol. Sci.* **4** 385–90
[29] Holroyd C B and Coles M G H 2002 The neural basis of human error processing: reinforcement learning, dopamine, and the error-related negativity *Psychol. Rev.* **109** 679–709
[30] Botvinick M M, Braver T S, Barch D M, Carter C S and Cohen J D 2001 Conflict monitoring and cognitive control *Psychol. Rev.* **108** 624–52
[31] Gentsch A, Ullsperger P and Ullsperger M 2009 Dissociable medial frontal negativities from a common monitoring system for self- and externally caused failure of goal achievement *NeuroImage* **47** 2023–30
[32] Ullsperger M and von Cramon D Y 2001 Subprocesses of performance monitoring: a dissociation of error processing and response competition revealed by event-related fMRI and ERPs *NeuroImage* **14** 1387–401
[33] Eriksen B A and Eriksen C W 1974 Effects of noise letters upon the identification of a target letter in a nonsearch task *Percept. Psychophys.* **16** 143–9
[34] Steinhauser R and Steinhauser M 2021 Adaptive rescheduling of error monitoring in multitasking *NeuroImage* **232** 117888
[35] Bilder R M, Lencz T, Ashtari M and Turkel E 1998 Left paleocortical activation by an alternating "Go/No-Go" task *NeuroImage* **7** S882
[36] Brázdil M, Roman R, Daniel P and Rektor I 2005 Intracerebral error-related negativity in a simple Go/NoGo task *J. Psychophysiol.* **19** 244–55
[37] Sun J, Huang J, Wang A, Zhang M and Tang X 2022 The role of the interaction between the inferior parietal lobule and superior temporal gyrus in the multisensory Go/No-go task *NeuroImage* **254** 119140
[38] Vocat R, Pourtois G and Vuilleumier P 2008 Unavoidable errors: a spatio-temporal analysis of time-course and neural sources of evoked potentials associated with error processing in a speeded task *Neuropsychologia* **46** 2545–55
[39] Egner T and Hirsch J 2005 The neural correlates and functional integration of cognitive control in a Stroop task *NeuroImage* **24** 539–47
[40] MacLeod C M 1991 Half a century of research on the Stroop effect: an integrative review *Psychol. Bull.* **109** 163–203
[41] Meyer A, Riesel A and Proudfit G H 2013 Reliability of the ERN across multiple tasks as a function of increasing errors *Psychophysiology* **50** 1220–5
[42] Endrass T, Reuter B and Kathmann N 2007 ERP correlates of conscious error recognition: aware and unaware errors in an antisaccade task *Eur. J. Neurosci.* **26** 1714–20
[43] Nieuwenhuis S, Richard Ridderinkhof K, Blom J, Band G P H and Kok A 2001 Error-related brain potentials are differentially related to awareness of response errors: evidence from an antisaccade task *Psychophysiology* **38** 752–60
[44] Steinhauser M and Yeung N 2010 Decision processes in human performance monitoring *J. Neurosci.* **30** 15643–53
[45] Hester R, Foxe J J, Molholm S, Shpaner M and Garavan H 2005 Neural mechanisms involved in error processing: a comparison of errors made with and without awareness *NeuroImage* **27** 602–8
[46] Ridderinkhof K R, Ramautar J R and Wijnen J G 2009 To PE or not to PE: a P3-like ERP component reflecting the processing of response errors *Psychophysiology* **46** 531–8
[47] Mochizuki G, Boe S, Marlin A and McIlroy W E 2010 Perturbation-evoked cortical activity reflects both the context and consequence of postural instability *Neuroscience* **170** 599–609
[48] Hajcak G, Moser J S, Yeung N and Simons R F 2005 On the ERN and the significance of errors *Psychophysiology* **42** 151–60
[49] Mierau A, Hülsdünker T and Strüder H K 2015 Changes in cortical activity associated with adaptive behavior during repeated balance perturbation of unpredictable timing *Front. Behav. Neurosci.* **9** 272
[50] Peterson S M and Ferris D P 2019 Group-level cortical and muscular connectivity during perturbations to walking and standing balance *NeuroImage* **198** 93–103
[51] Solis-Escalante T, van der Cruijsen J, de Kam D, van Kordelaar J, Weerdesteyn V and Schouten A C 2019 Cortical dynamics during preparation and execution of reactive balance responses with distinct postural demands *NeuroImage* **188** 557–71
[52] Brown J W and Braver T S 2005 Learned predictions of error likelihood in the anterior cingulate cortex *Science* **307** 1118–21
[53] Carter C S, Braver T S, Barch D M, Botvinick M M, Noll D and Cohen J D 1998 Anterior cingulate cortex, error detection, and the online monitoring of performance *Science* **280** 747–9
[54] Ferrez P W and Millan J D 2008 Error-related EEG potentials generated during simulated brain–computer interaction *IEEE Trans. Biomed. Eng.* **55** 923–9
[55] Jessup R K, Busemeyer J R and Brown J W 2010 Error effects in anterior cingulate cortex reverse when error likelihood is high *J. Neurosci.* **30** 3467–72
[56] O'Connell R G, Dockree P M, Bellgrove M A, Kelly S P, Hester R, Garavan H, Robertson I H and Foxe J J 2007 The role of cingulate cortex in the detection of errors with and without awareness: a high-density electrical mapping study *Eur. J. Neurosci.* **25** 2571–9
[57] Fitzgerald K D, Perkins S C, Angstadt M, Johnson T, Stern E R, Welsh R C and Taylor S F 2010 The development of performance-monitoring function in the posterior medial frontal cortex *NeuroImage* **49** 3463–73
[58] Izuma K 2013 The neural basis of social influence and attitude change *Curr. Opin. Neurobiol.* **23** 456–62
[59] Ridderinkhof K R, Ullsperger M, Crone E A and Nieuwenhuis S 2004 The role of the medial frontal cortex in cognitive control *Science* **306** 443–7
[60] Kothe C*et al* 2019 (available at: https://labstreaminglayer.org/#/)
[61] Delorme A and Makeig S 2004 EEGLAB: an open source toolbox for analysis of single-trial EEG dynamics including independent component analysis *J. Neurosci. Methods* **134** 9–21
[62] Tadel F, Baillet S, Mosher J C, Pantazis D and Leahy R M 2011 Brainstorm: a user-friendly application for MEG/EEG analysis *Comput. Intell. Neurosci.* **2011** 879716

[63] Oostenveld R, Fries P, Maris E and Schoffelen J-M 2011 FieldTrip: open source software for advanced analysis of MEG, EEG, and invasive electrophysiological data *Comput. Intell. Neurosci.* **2011** 156869
[64] Mullen T, Kothe C, Chi Y M, Ojeda A, Kerth T, Makeig S, Cauwenberghs G and Jung T-P 2013 Real-time modeling and 3D visualization of source dynamics and connectivity using wearable EEG *2013 35th Annual Int. Conf. of the IEEE Engineering in Medicine and Biology Society (EMBC)* (Osaka: IEEE) pp 2184–7
[65] Artoni F, Fanciullacci C, Bertolucci F, Panarese A, Makeig S, Micera S and Chisari C 2017 Unidirectional brain to muscle connectivity reveals motor cortex control of leg muscles during stereotyped walking *NeuroImage* **159** 403–16
[66] Goel R, Nakagome S, Rao N, Paloski W H, Contreras-Vidal J L and Parikh P J 2019 Fronto-parietal brain areas contribute to the online control of posture during a continuous balance task *Neuroscience* **413** 135–53
[67] Pion-Tonachini L, Kreutz-Delgado K and Makeig S 2019 ICLabel: an automated electroencephalographic independent component classifier, dataset, and website *NeuroImage* **198** 181–97
[68] Maris E and Oostenveld R 2007 Nonparametric statistical testing of EEG- and MEG-data *J. Neurosci. Methods* **164** 177–90
[69] Kalcher J and Pfurtscheller G 1995 Discrimination between phase-locked and non-phase-locked event-related EEG activity *Electroencephalogr. Clin. Neurophysiol.* **94** 381–4
[70] Gramfort A, Papadopoulo T, Olivi E and Clerc M 2010 OpenMEEG: opensource software for quasistatic bioelectromagnetics *Biomed. Eng. OnLine* **9** 45
[71] Pascual-Marqui R D 2002 Standardized low-resolution brain electromagnetic tomography (sLORETA): technical details *Methods Find. Exp. Clin. Pharmacol.* **24** 5–12
[72] Marlin A, Mochizuki G, Staines W R and McIlroy W E 2014 Localizing evoked cortical activity associated with balance reactions: does the anterior cingulate play a role? *J. Neurophysiol.* **111** 2634–43
[73] Lopez-Larraz E, Iturrate I, Montesano L and Minguez J 2010 Real-time recognition of feedback error-related potentials during a time-estimation task *2010 Annual Int. Conf. of the IEEE Engineering in Medicine and Biology* pp 2670–3
[74] Lopes-Dias C, Sburlea A I, Breitegger K, Wyss D, Drescher H, Wildburger R and Müller-Putz G R 2021 Online asynchronous detection of error-related potentials in participants with a spinal cord injury using a generic classifier *J. Neural Eng.* **18** 046022
[75] Roset S A, Gant K, Prasad A and Sanchez J C 2014 An adaptive brain actuated system for augmenting rehabilitation *Front. Neurosci.* **8** 415
[76] Olvet D M and Hajcak G 2009 The stability of error-related brain activity with increasing trials *Psychophysiology* **46** 957–61
[77] van Schie H T, Mars R B, Coles M G and Bekkering H 2004 Modulation of activity in medial frontal and motor cortices during error observation *Nat. Neurosci.* **7** 549–54
[78] Cavanagh J F, Zambrano-Vazquez L and Allen J J 2012 Theta lingua franca: a common mid-frontal substrate for action monitoring processes *Psychophysiology* **49** 220–38
[79] Yordanova J, Falkenstein M, Hohnsbein J and Kolev V 2004 Parallel systems of error processing in the brain *NeuroImage* **22** 590–602
[80] Luu P, Tucker D M and Makeig S 2004 Frontal midline theta and the error-related negativity: neurophysiological mechanisms of action regulation *Clin. Neurophysiol.* **115** 1821–35
[81] Carp J and Compton R J 2009 Alpha power is influenced by performance errors *Psychophysiology* **46** 336–43
[82] Compton R J, Arnstein D, Freedman G, Dainer-Best J and Liss A 2011 Cognitive control in the intertrial interval: evidence from EEG alpha power *Psychophysiology* **48** 583–90
[83] Klimesch W, Doppelmayr M, Russegger H, Pachinger T and Schwaiger J 1998 Induced alpha band power changes in the human EEG and attention *Neurosci. Lett.* **244** 73–76
[84] Compton R J, Gearinger D, Wild H, Rette D, Heaton E C, Histon S, Thiel P and Jaskir M 2021 Simultaneous EEG and pupillary evidence for post-error arousal during a speeded performance task *Eur. J. Neurosci.* **53** 543–55
[85] Navarro-Cebrian A, Knight R T and Kayser A S 2013 Error-monitoring and post-error compensations: dissociation between perceptual failures and motor errors with and without awareness *J. Neurosci.* **33** 12375–83
[86] van Driel J, Ridderinkhof K R and Cohen M X 2012 Not all errors are alike: theta and alpha EEG dynamics relate to differences in error-processing dynamics *J. Neurosci.* **32** 16795–806
[87] Mazaheri A, Nieuwenhuis I L C, van Dijk H and Jensen O 2009 Prestimulus alpha and mu activity predicts failure to inhibit motor responses *Hum. Brain Mapp.* **30** 1791–800
[88] Badgaiyan R D and Posner M I 1998 Mapping the cingulate cortex in response selection and monitoring *NeuroImage* **7** 255–60
[89] Cavanna A E and Trimble M R 2006 The precuneus: a review of its functional anatomy and behavioural correlates *Brain J. Neurol.* **129** 564–83
[90] Menon V, Adleman N E, White C D, Glover G H and Reiss A L 2001 Error-related brain activation during a Go/NoGo response inhibition task *Hum. Brain Mapp.* **12** 131–43
[91] Matthews S C, Simmons A N, Arce E and Paulus M P 2005 Dissociation of inhibition from error processing using a parametric inhibitory task during functional magnetic resonance imaging *NeuroReport* **16** 755–60